Title
Methods for CT Automatic Exposure Control Protocol Translation Between Scanner Platforms

Journal
Journal of the American College of Radiology, 11(3)

ISSN
1546-1440

Authors
McKenney, Sarah E
Seibert, J Anthony
Lamba, Ramit
et al.

Publication Date
2014-03-01

DOI
10.1016/j.jacr.2013.10.014

Peer reviewed

Published in final edited form as:
J Am Coll Radiol. 2014 March ; 11(3): 285–291. doi:10.1016/j.jacr.2013.10.014.

Methods for CT Automatic Exposure Control Protocol Translation between Scanner Platforms

Sarah E. McKenney, Ph.D., **J. Anthony Seibert, Ph.D.**, **Ramit Lamba, M.D.**, and **John M. Boone, Ph.D.**
Department of Radiology, University of California Davis Medical Center, Sacramento, California

Abstract

Purpose—An imaging facility with a diverse fleet of CT scanners faces considerable challenges when propagating CT protocols with consistent image quality and patient dose across scanner makes and models. While some protocol parameters can comfortably remain constant between scanners (*e.g*. kV, gantry rotation time, *etc*.), the automatic exposure control parameter, which selects the overall mA level during tube current modulation, is difficult to match between scanners, especially from different CT manufacturers.

Method—Objective methods for converting tube-current-modulation protocols between CT scanners were developed. Three CT scanners were investigated, a GE LightSpeed 16 scanner, a GE VCT scanner, and a Siemens Definition AS+ scanner. Translation of the automatic exposure control (AEC) parameters such as noise index or quality reference mAs across CT scanners was specifically investigated. A variable-diameter polymethyl methacrylate (PMMA) phantom was imaged on the three scanners using a range of AEC parameters for each scanner. The phantom consisted of 5 cylindrical sections with diameters of 13 cm, 16 cm, 20 cm, 25 cm, and 32 cm. The protocol translation scheme was based upon matching either the $CTDI_{vol}$ or image noise (in HU) between two different CT scanners. A series of analytical fit functions, corresponding to different patient sizes (phantom diameters) were developed from the measured CT data. These functions relate the AEC metric of the reference scanner, the GE LightSpeed 16 in this case, to the AEC metric of a secondary scanner.

Results—When translating protocols between different models of CT scanners (from the GE LightSpeed 16 reference scanner to the GE VCT system), the translation functions were linear. However, a power-law function was necessary to convert the AEC functions of the GE LightSpeed 16 reference scanner to the Siemens Definition AS+ secondary scanner, due to differences in the AEC functionality designed by these two companies.

Conclusions—Protocol translation based on quantitative metrics – volume computed tomography dose index or measured image noise is feasible. Protocol translation has a dependency on patient size, especially between the GE and Siemens' systems. Translation schemes that preserve dose levels may not produce identical image quality.

Corresponding Author: John M. Boone, University of California Davis Medical Center, 4860 Y Street, Ellison Building Suite 3100, Sacramento, CA 95817 jmboone@ucdavis.edu.

Keywords

CT protocols; Automatic Exposure Control; Tube Current Modulation; Phantoms

INTRODUCTION

The development of CT protocols on a given scanner requires significant technical familiarity with computed tomography, and a great deal of clinical experience as a radiologist to determine the optimal trade-off between adequate diagnostic image quality and low radiation dose. Furthermore, a large number of different protocols are used on any modern CT scanner, specific to head, chest, abdomen/pelvis, and other niche imaging applications. It is not uncommon for a clinical CT scanner to have 200 to 300 protocols loaded onto it, of which perhaps 20 are used with frequency.

Because CT scanners are important diagnostic workhorses at most medical centers, the number of CT scanners at each institution can range from 1-3 for small facilities to 30 or more, for large regional health systems. In such an environment, there is usually a range of different types of CT scanners, typically different models from the same commercial vendor and often CT scanners from several different vendors are located at a given institution. This heterogeneity reflects changes in purchasing preferences over the lifetime of the CT scanner inventory. In this common situation, radiologists (with CT technologists and medical physicists) are faced with the challenge of converting existing, well-established CT protocols from one CT scanner to different scanners – in some cases newer scanners from the same CT manufacturer, and in some cases new scanners from different manufacturers. Because it is unrealistic to develop a complete set of new CT protocols for every type of CT scanner which is available at a given institution, it is useful to have a method by which CT protocols from one scanner (here, referred to as the *reference* scanner) to one or more *secondary* CT scanner systems.

In the era when fixed x-ray tube current protocols were common, translating CT protocols based upon similar dose metric levels was relatively straightforward. However, automatic exposure control (AEC) with x-ray tube current modulation (TCM) is now widely used in CT, especially in thoracic and abdomen pelvis CT applications[1]. With the use of automatic exposure control, protocol translation becomes much more complicated, especially between different CT manufacturers[2][3].

Developing objective methods to translate CT protocols from one scanner to another requires that either radiation dose levels or CT image quality (essentially image noise) be used as the translational metric - that is, the parameter that is held constant as a CT protocol is propagated from one scanner to another. In this study, radiation dose levels were quantified using the volume computed tomography dose index ($CTDI_{vol}$), which is a ubiquitous quantity that is reported by all modern CT scanners on the operator's console. If radiation dose levels are kept constant through the protocol conversion exercise, the assumption is that similar image quality levels (between the reference scanner and the secondary scanner) will result. There are a number of assumptions (similar reconstruction kernels, reconstructed slice thicknesses, reconstructed field of view, etc.) required for this to be true, but in principle this is a reasonable assumption.

Another approach to matching protocols between different CT scanners is to attempt to maintain the same image quality (noise, as measured by the standard deviation in Hounsfield units- σ_{HU}) as a given protocol is translated from the reference to the secondary scanner. This approach is tailored more towards matching the appearance of images as seen by the radiologist, but is also dependent upon the selection of similar reconstruction kernels (and whether or not iterative reconstruction techniques are used) between CT scanners.

In this investigation, radiation dose levels as quantified by $CTDI_{vol}$, and image quality (as quantified by σ_{HU}) were used to develop conversion techniques between protocols between one reference scanner and two different secondary CT systems.

METHODS

The translation scheme used in this study assumes that there is a reference scanner with a list of well-established protocols, and the goal is then to translate these protocols to a secondary CT scanner, of different make and/or model. The focus of this effort is to develop automatic exposure control parameters which match either "dose" ($CTDI_{vol}$) or measured image noise between scanners.

The Phantom

A variable-diameter ("wedding cake") phantom was constructed from five polymethyl methacrylate (PMMA) cylindrical phantoms (Figure 1A). Each phantom had a length of 15 cm; the physical phantom diameters were 13 cm, 16 cm, 20 cm, 25 cm, and 32 cm. When the density of PMMA (ρ = 1.19 g/cm^2) is factored in, the phantoms had water-equivalent diameters of 15 cm, 18 cm, 22 cm, 27 cm, and 34 cm, approximating the patient diameters from a newborn to a large adult. The phantoms were stacked longitudinally and held together in tension with a PMMA rod through a centering hole. The central axis of the phantom was positioned at the system's isocenter with the small diameter phantoms supported with foam blocks. The phantom was oriented such that the 32 cm cylinder was at the "head" position of the table and the 13 cm phantom was at the "feet" position.

CT Scanners

The phantom was imaged on three clinical CT scanners. The reference scanner was a GE LightSpeed 16 (General Electric Medical Systems, Waukesha, Wisconsin), which contains an extensive set of patient protocols developed by the chief CT radiologist at our institution. One secondary scanner was a GE VCT (General Electric Medical Systems, Waukesha, Wisconsin) and the other secondary scanner was a Siemens Definition 128 AS+ (Siemens Medical Systems, Erlangen, Germany).

The standard abdomen/pelvis protocol at 120 kV was used on all scanners. Details of the technique factors are provided in Table I. Several parameters were held constant between protocols; the tube potential was set to 120 kV in all cases, and all images were reconstructed with a 400 mm field of view (FOV) and a slice thickness of 5 mm. The standard kernel was used on the GE scanners and the B40 kernel was used on the Siemens scanner. The large body bow tie filter was used in all cases. On each scanner, the phantom was imaged repeatedly over a wide range of AEC parameter values – *noise index* on the GE systems, and the *quality reference mAs* on the Siemens scanner.

The AEC metric on a GE scanners, the noise index, was designed by the manufacturer to be directly proportional to image noise. The tube current range was 100 mA to 440 mA on the Lightspeed 16 and 100 mA to 600 mA on the VCT; however, the tube current modulation scheme would reach a minimum mA for smaller phantoms with high noise index values or would hit a maximum mA for larger phantoms with low noise index values. Consequently, only regions within the phantom where the tube current could accurately be modulated were selected and scanned for this study – scans which exceeded the dynamic range of the scanners were discarded. The noise index values investigated were 3, 4, 4.5, 5.5, 8, 12, 15, 20, 25, 30, 40, and 60.

The AEC metric on a Siemens scanner, the quality reference mAs[4], was designed by the vendor to be directly proportional to the tube current-time product, i.e. mAs. The tube current modulated across the entire phantom; thus the entire phantom was scanned at quality reference mAs values of 50, 100, 200, 300, 400, 500, and 600.

Computational Implementation

A computer program with a graphical user interface was developed on MatLab (The MathWorks, Inc., Natick, Massachusetts) to determine the average effective mAs for each phantom diameter (Figure 1B). The effective mAs was defined as the actual mAs value, divided by the pitch factor; effective mAs = mAs / pitch. The program read and then displayed the images from each phantom CT scan. Water-equivalent diameter [5-7], and other metrics were computed as well. Orthogonal projection images were computed from the CT data sets and displayed, and pertinent scan identifiers and parameters (read from the DICOM header), were displayed as well. For noise assessment, manually-selected regions within the images were placed. Regions with a relatively constant tube current within a single phantom were selected.

Translation with $CTDI_{vol}$

$CTDI_{vol}$[8] was used to match CT output between scanners. $CTDI_{vol}$ at a fixed x-ray tube current setting (*i.e*. mGy/100 mAs) was used as a surrogate for tube output as it includes the effects of scanner geometry, source to isocenter distance, bow-tie filter shape, pitch, and spectral effects - unlike the effective mAs. $CTDI_{vol}$, which is measured using a phantom, also includes the scattering effects of the dose delivered to a phantom. The radiation dose of the reference scanner was obtained by scaling $CTDI_{vol}$ by the average effective mAs for each image in a given region of the phantom corresponding to a specific diameter (13-32 cm). The effective mAs $\mathscr{E}$ of the secondary scanner that delivers the same $CTDI_{vol}$ per 100 mAs was then estimated by

$$\mathscr{E}_{secondary}=\mathscr{E}_{reference}\frac{\left[CTDI_{\text{vol}}^{@100\text{ mAs}}\right]_{reference}}{\left[CTDI_{\text{vol}}^{@100\text{ mAs}}\right]_{secondary}}$$

Translation with image noise

The image noise was assessed from an annular region of interest (ROI) through the entire length of the phantom. The ROI was centered within the phantom, but excluded the centering rod (see inset on Figure 2B). The ROI had an inner diameter of 23 mm and an outer diameter of 47 mm. For each phantom diameter, the ROI was located in the same position for consistency [9, 10].

The image noise was calculated as the standard deviation of Hounsfield Units within the ROI; σ_{HU}. The image noise was then averaged across all the slices within a manually selected region using the GUI shown in Figure 1A.

RESULTS

Data from the 32 cm diameter phantom only

The acquired data associated with the 32 cm diameter PMMA phantom is illustrated in Figure 2A. Here, $CTDI_{vol}$ is shown as a function of noise index for the GE CT scanners

(Lightspeed 16 and VCT, bottom axis) and as a function of quality reference mAs (top axis) of the Siemens CT system. Because the Siemens system uses an automatic exposure control parameter (the *quality reference mAs*) related to mAs (and thus $CTDI_{vol}$), it is not surprising that there is a linear relationship between these parameters. The GE scanners, however, utilize an automatic exposure control parameter (*noise index*) which is related to image noise, which in turn is related approximately to the inverse of the square root of the effective mAs ($mAs^{-0.5}$) or $CTDI_{vol}$. Therefore, there is a nonlinear relationship between the noise index and the $CTDI_{vol}$, and this is evident in the figure.

Acquired image data was evaluated to assess image noise, for the 32 cm diameter PMMA phantom (Figure 2B). In this figure, the quality reference mAs of the Siemens scanner is seen to be non-linearly related to image noise. While the relationship between the noise index from the 2 GE scanners and measured image noise is not perfectly linear, these values are proportionate to each other with some slight nonlinear trends.

The data from the 32 cm diameter phantom is shown in Figure 3A, where the noise index of the GE VCT scanner is plotted as a function of the noise index of the GE Lightspeed-16 system. These values show a reasonable 1:1 ratio (unity slope, zero offset) when the $CTDI_{vol}$ is plotted, however there is a non-unity slope which defines the approximately linear relationship when measured image noise is used for the comparison. This figure illustrates quite literally the relationship between the noise index of the secondary scanner (on the y-axis) as a function of the noise index of the reference scanner (on the x-axis).

The relationship between the Siemens AS+ scanner performance and that of the GE Lightspeed-16 system is shown in Figure 3B, for the 32 cm diameter phantom. The relationship is shown for both the measured noise and measured $CTDI_{vol}$ values. Here, there is a nonlinear relationship. As the GE system's noise index is reduced, the quality reference mAs (Siemens system) has to be increased exponentially to produce the same image quality (noise) or dose ($CTDI_{vol}$), and this is a consequence of how each vendor has designed their automatic exposure control parameter.

Protocol translation between models (GE Lightspeed → GE VCT)

An example of protocol matching between the GE LightSpeed 16 reference scanner and the GE VCT secondary scanner for the minimum (13 cm) and maximum (32 cm) phantom diameters is illustrated in Figure 4A using the $CTDI_{vol}$ metric, and in Figure 4B, using the image noise metric. The translation functions between the two GE scanners were linearly proportional and a series of linear functions ($Y = aX + b$) were developed for all five phantom diameters (Table 2) using linear regression. The slope of the translation function increased as phantom diameter decreased. The translation scheme matching noise (Figure 4B) exhibited the opposite trend, where the slope increased for phantoms with larger diameters. In both cases, the differences in the relationships as a function of phantom diameter were relatively small.

Protocol translation between manufacturers (GE Lightspeed → Siemens AS+)

The translation of the AEC metric of the GE LightSpeed 16 reference scanner to the Siemens AS+ secondary scanner using both $CTDI_{vol}$ (Figure 5A) and image noise (Figure 5B) parameters were described by power functions of the form $Y = aX^b + c$. The quality reference mAs increased for a given noise index as the phantom diameter increased. The parameters of the equations describing each of these curves (and for the intermediate diameter phantoms) are provided in Table 2.

DISCUSSION

The process of developing uniform CT protocols across an entire fleet of CT scanners at a given institution is potentially daunting. In this investigation, phantom measurements combined with a quantitative construct were used to develop equations which can be used to adjust AEC parameters between CT scanners of different model types and different manufacturers. It should be noted that the precise equations and constants described in this work may not accurately predict the appropriate translation for similar types of CT scanners; the purpose here was to demonstrate the method, not to provide the precise functional relationship between the CT scanners studied here.

Determining the appropriate AEC parameter between scanners is only one of many factors which go into a specific CT protocol. Many other parameters also need to be considered. For example, the GE Lightspeed-16 used in this investigation has a maximum collimation width of 20 mm, while the GE VCT scanner has a maximum collimation width of 40 mm. For the same gantry rotation time and pitch, the VCT system will scan the patient in half the time. This suggests that the timing of contrast injection protocols need to be significantly adjusted. Other parameters such as x-ray tube potential, bowtie factor, gantry rotation period, reconstruction filter, patient dimensions, *etc*. will in most cases need to be evaluated when converting protocols from one scanner to another.

The use of iterative reconstruction (IR) methods offers considerable reduction in patient dose[11], however matching the performance of iterative reconstruction methods between CT scanners of different manufacturers will pose additional challenges in the context of transferring protocols between scanners. The issue is made even more complex in that different mixtures (between filtered backprojection and IR algorithms) and different generations of iterative reconstruction algorithm are available from most CT vendors.

In this investigation, two different parameters: image noise and $CTDI_{vol}$ were used as objective metrics for converting AEC protocols between two different types of CT scanners. It is observed that the use of the $CTDI_{vol}$ dose metric is probably the most straightforward approach, and it can be independently quantified by making dose measurements. The use of the image quality parameter, σ_{HU}, especially between CT scanners from different manufacturers, is made more complicated by the different reconstruction kernels used by each manufacturer. Towards this end, Solomon *et al*. [12] have compared the noise texture between General Electric and Siemens CT scanner kernels, and their work provides excellent guidance in terms of matching reconstruction kernels between these two manufacturers.

The objective methods for protocol translation described in this study are mathematical in construct. For an institution with many CT scanners (*e.g*., ≥5), the use of spreadsheet programs (with the ability to perform mathematical operations between cells) for CT protocols would enable relatively easy propagation of CT protocols from a reference CT scanner to one or more secondary CT systems. In the future, it is anticipated that many other objective (and mathematical) protocol conversion methods will be developed for other protocol parameters including kV, reconstruction field of view, slice thickness, *etc*.

CONCLUSIONS

The task of CT protocol translation between two different scanners is formidable; however, this investigation does provide guidance as to an objective methodology for calibrating AEC parameters between scanners. It is likely that due to slight differences between individual CT scanners - even of the same make and model, that individual translation curves will need to be developed for each make and model of CT scanner at a given institution. Nevertheless, the methods described herein are straightforward and are relatively easy to implement assuming the presence of appropriate phantoms and appropriately trained individuals.

Acknowledgments

Partial funding from grants from the University of California Davis Health System, the University of California Office of the President Center for Health Quality and Innovation Award, and NIH R01 EB002138 is gratefully acknowledged.

REFERENCES

1. McCollough CH. Automatic exposure control in CT: Are we done yet? Radiology. Jan.2006 237:755–756. [PubMed: 16304094]
2. CT Scan Protocols. Apr 1. 2013 Available: http://www.aapm.org/pubs/CTProtocols/
3. Kofler, JM.; McCollough, CH.; Vrieze, TJ.; Bruesewitz, MR.; Yu, L.; Leng, SA. Team-based methods for effectively creating, managing and distributing CT protocols. 2010. Available: http://mayoresearch.mayo.edu/mayo/research/ctcic/upload/2010-rsna-kofler.pdf
4. Angel E, Yaghmai N, Jude CM, DeMarco JJ, Cagnon CH, Goldin JG, et al. Dose to Radiosensitive Organs During Routine Chest CT: Effects of Tube Current Modulation. American Journal of Roentgenology. Nov.2009 193:1340–1345. [PubMed: 19843751]
5. T. G. 204. American Association of Physicists in Medicine. Vol. 204. College Park: 2011. Size-Specific Dose Estimates (SSDE) in Pediatric and Adult Body CT Examinations.
6. Wang J, Christner JA, Duan X, Leng S, Yu L, McCollough CH. Attenuation-based estimation of patient size for the purpose of size specific dose estimation in CT. Part II. Implementation on abdomen and thorax phantoms using cross sectional CT images and scanned projection radiograph images. Medical Physics. Nov.2012 39:6772–6778. [PubMed: 23127071]
7. Wang J, Duan X, Christner JA, Leng S, Yu L, McCollough CH. Attenuation-based estimation of patient size for the purpose of size specific dose estimation in CT. Part I. Development and validation of methods using the CT image. Medical Physics. Nov.2012 39:6764–6771. [PubMed: 23127070]
8. Leitz W, Axelsson B, Szendro G. COMPUTED-TOMOGRAPHY DOSE ASSESSMENT - A PRACTICAL APPROACH. Radiation Protection Dosimetry. 1995; 57:377–380.
9. Pineda AR, Siewerdsen JH, Tward DJ. Analysis of image noise in 3D cone-beam CT: spatial and Fourier domain approaches under conditions of varying stationarity. :69131Q–69131Q, 2008.
10. Pineda AR, Tward DJ, Gonzalez A, Siewerdsen JH. Beyond noise power in 3D computed tomography: The local NPS and off-diagonal elements of the Fourier domain covariance matrix. Medical Physics. Jun.2012 39:3240–3252. [PubMed: 22755707]
11. Silva AC, Lawder HJ, Hara A, Kujak J, Pavlicek W. Innovations in CT Dose Reduction Strategy: Application of the Adaptive Statistical Iterative Reconstruction Algorithm. American Journal of Roentgenology. Jan.2010 194:191–199. [PubMed: 20028923]
12. Solomon JB, Christianson O, Samei E. Quantitative comparison of noise texture across CT scanners from different manufacturers. Medical Physics. Oct.2012 39:6048–6055. [PubMed: 23039643]

3 to 6 take-home points

- The AEC control parameters between GE CT scanners (Noise Index) and Siemens CT scanners (quality reference mAs) are non-linearly related, but a power function describes the conversion process well.
- Measurements across a range of AEC parameters performed using a multi-tiered phantom (with segments of different diameters) provide the raw data which is necessary to objectively convert AEC parameters from one scanner type to another.
- Two approaches are described, where either the image quality (measured noise in the phantom images) or radiation dose (as defined by the CTDIvol) are matched between scanners.
- As we enter an era where CT protocols are more complex and need to be frequently adjusted across all of the scanners at an institution, having CT protocols defined within a spreadsheet or data base programs where calculations can be performed will allow an institution to more quickly adapt CT protocols using objective methods such as those described in this paper.

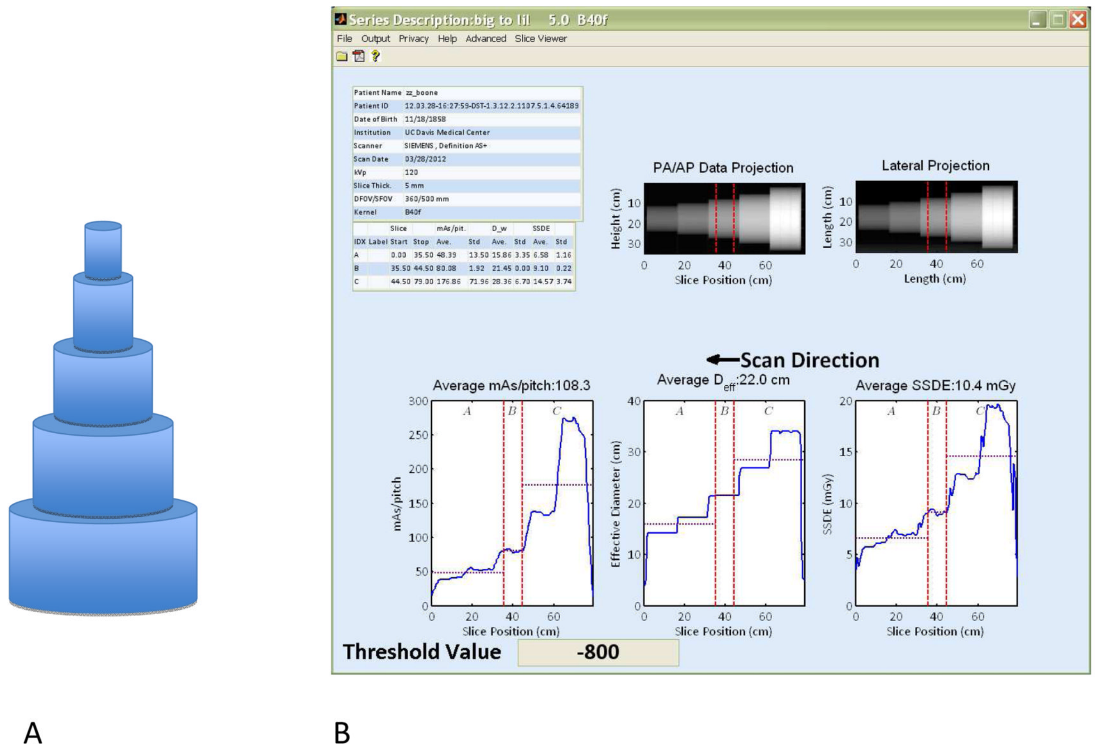

Figure 1.

A: The variable diameter “wedding cake” phantom is illustrated

Figure 1B: The graphic user interface, developed in Matlab, is shown. This tool was used for image analysis and averaging DICOM values across phantom diameters.

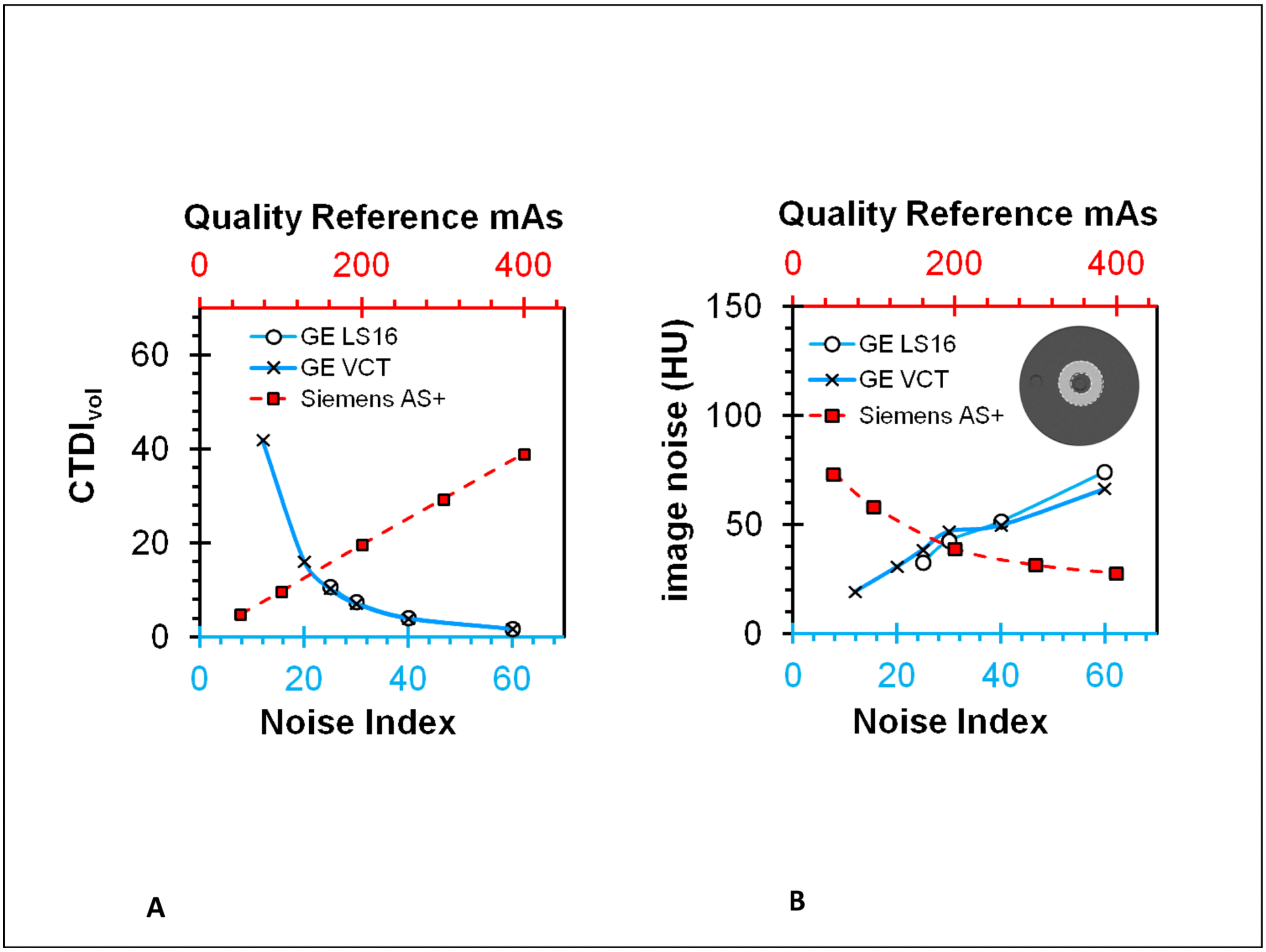

Figure 2.

A: The $CTDI_{vol}$ is shown as a function of noise index (bottom axis) and quality reference mAs (top axis), for the three CT scanners evaluated in this study.

Figure 2B: The measured image noise (in HU) is shown as a function of noise index (bottom axis) or quality reference mAs (top axis), for 3 CT systems.

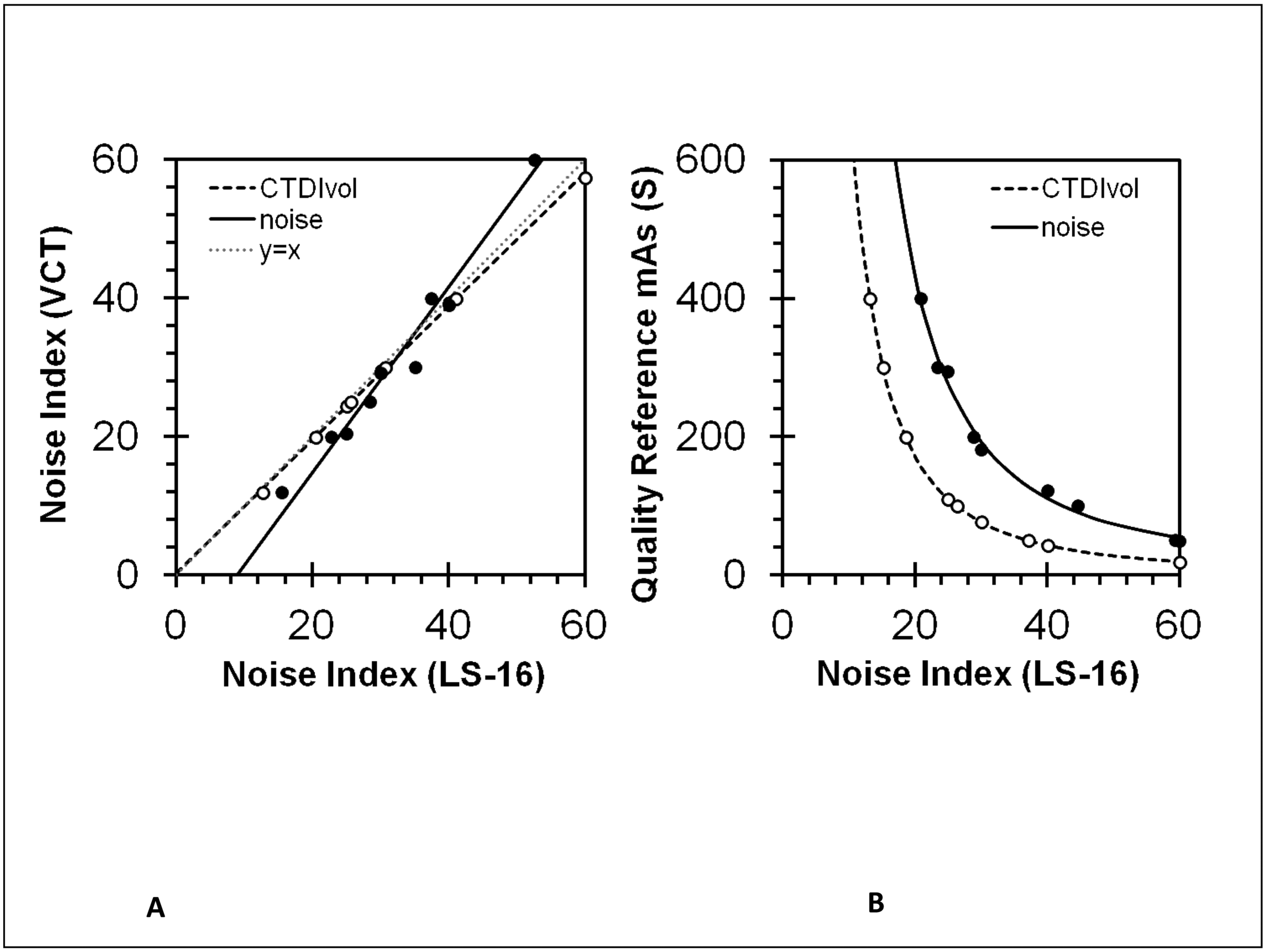

Figure 3.

A: The noise index of the GE VCT system is plotted on the vertical axis, and the noise index of the GE Lightspeed-16 system is plotted on the horizontal axis. The corresponding measured values produced by these AEC parameters, the $CTDI_{vol}$ and measured image noise, form the two plots. This plot shows data measured from the 32 cm diameter PMMA phantom.

Figure 3B: The measured values of $CTDI_{vol}$ and image noise are plotted for the AEC settings (quality reference mAs) on the Siemens' scanner (vertical axis) and the GE Lightspeed-16 system (horizontal axis). Data from the 32 cm diameter phantom is shown.

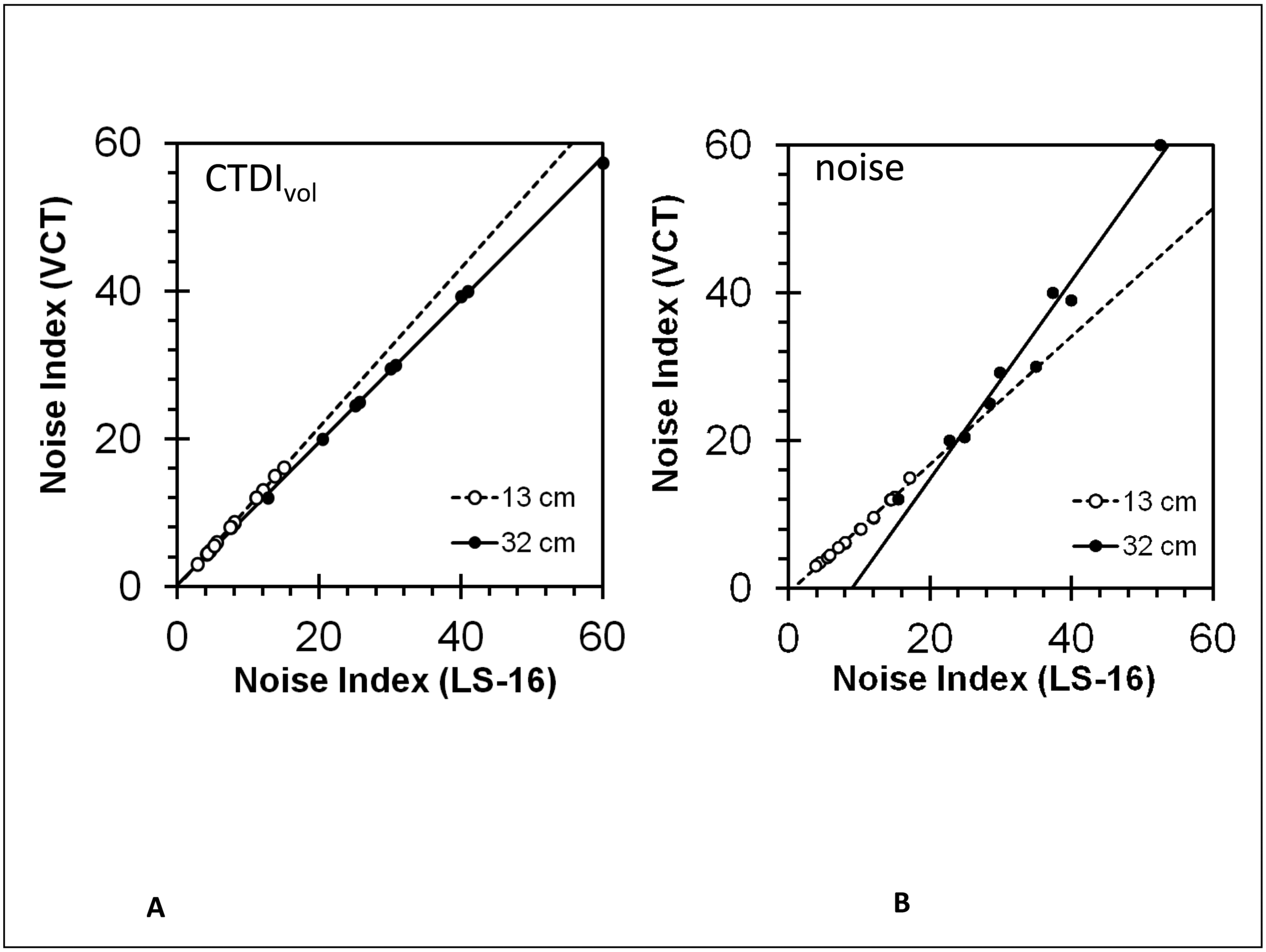

Figure 4.

A: The best-matched noise index parameter for the GE VCT system is plotted as a function of the noise index for the Lightspeed-16 system, for 2 phantom diameters (as indicated). These curves demonstrate the use of $CTDI_{vol}$ as the parameter to keep constant during protocol translation. These curves represent the translation curves by which the reference values of the LS-16 system can be converted to noise index values on the VCT system. Table 2 shows curve-fit parameters for all 5 phantom diameters evaluated.

Figure 4B: The translation curves are shown from the LS-16 system to the VCT scanner, keeping image noise constant. Table 2 shows the fit coefficients for all 5 phantom diameters.

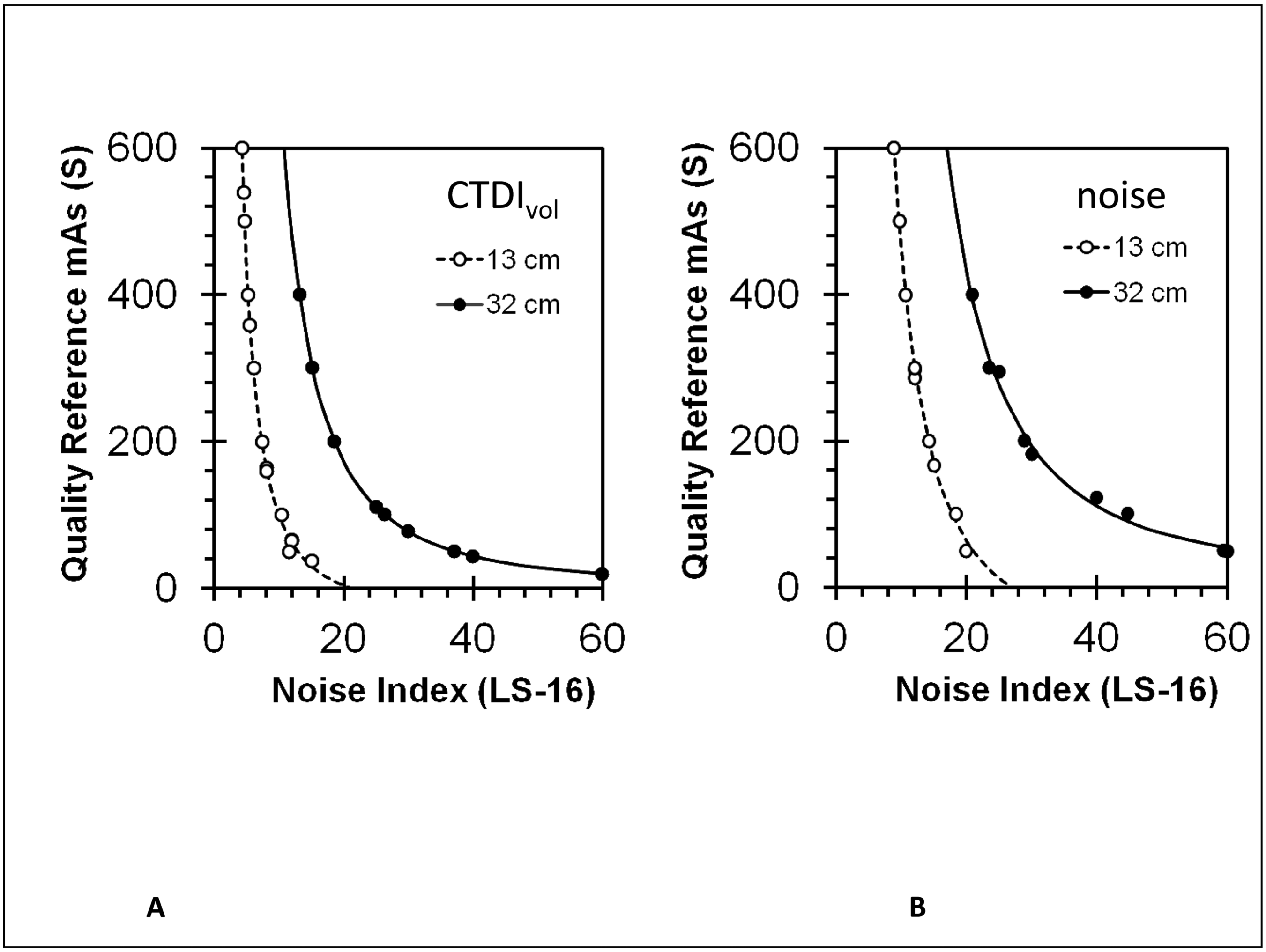

Figure 5.

A: The curves shown in this figure show the quality reference mAs on the Siemen's AS+ system which match the $CTDI_{vol}$ of the LS-16 system at a given noise index setting. Curve parameters (for all 5 phantom diameters) are shown in Table 2. The curves for the intermediate phantom diameters (16, 20, 25 cm) fall sequentially and between the two curves shown, but were not plotted for clarity.

Figure 5B: These curves show the quality reference mAs values for the Siemens AS+ which correspond to the noise index values of the GE LS-16 value, when measured image noise is used for the matching parameter. The fit parameters for all 5 phantom diameters are listed in Table 2.

NIH-PA Author Manuscript

NIH-PA Author Manuscript

Table 1

Technique factors for the investigated CT scanners.

Scanner	Rotation time (s)	Beam width (mm)	Pitch	TCM Metric
GE LightSpeed 16	0.6	10	1.375	Noise Index
GE VCT	0.5	20	0.969	Noise Index
Siemens AS+	0.5	38.4	0.75	reference mAs

Table 2

Translation functions using either $CTDI_{vol}$ or image noise as the translation metric.

$CTDL_{vol}$							
	GE LS16 → VCT			**GE LS16 → Siemens AS+**			
	y=ax+b			**$y=ax^b+c$**			
phantom diameter	**a**	**b**	**r^2**	**a**	**b**	**c**	**r^2**
13	1.08	0.05	0.999	8.6×10^3	−1.8	-3.5×10^1	0.999
16	1.12	−0.01	0.999	1.1×10^4	−1.9	-1.4×10^1	0.999
20	0.98	0.59	0.998	1.6×10^4	−1.9	-1.9×10^0	0.999
25	0.99	0.59	0.998	2.1×10^4	−1.8	-8.6×10^0	0.999
32	0.97	0.27	0.999	7.2×10^4	−2.0	2.5×10^{-1}	0.999

Noise							
	GE LS16 → VCT			**GE LS16 → Siemens AS+**			
	y=ax+b			**$y=ax^b+c$**			
phantom diameter	**a**	**b**	**r^2**	**a**	**b**	**c**	**r^2**
13	0.87	−0.58	0.995	4.2E+04	−1.88	−8.6E+01	0.998
16	0.87	−0.43	0.998	7.1E+04	−2.14	−2.5E+01	0.999
20	0.93	−1.31	0.977	1.4E+05	−2.24	−2.5E+01	0.996
25	1.05	−3.87	0.990	9.5E+05	−2.81	−8.1E+00	0.999
32	1.34	−12.01	0.980	2.0E+05	−2.06	1.0E+01	0.990